V/*F* Control of Squirrel Cage Induction Motor Drives Without Flux or Torque Measurement Dependency

Walid Emar *walidemar@yahoo.com*
Electrical Engineering Department
Isra University
11622 Amman, Jordan

Hussein Sarhan *hussein_52@hotmail.com*
Mechatronics Engineering Department
Balqa' Applied University
Amman, Jordan

Rateb Al-Issa *ratebissa@yahoo.com*
Mechatronics Engineering Department
Balqa' Applied University
Amman, Jordan

Issam TTrad *Issam_161@yahoo.com*
Faculty of science and information
Jadara University
Irbid, Jordan

Mahmoud Awad *Dr_Awad_M@yahoo.com*
Electrical Engineering Department
Balqa' Applied University
Amman, Jordan

Abstract

Based on the popular constant volts per hertz principle, two improvement techniques are presented: keeping maximum torque constant or keeping magnetic flux constant. An open-loop inverter-three-phase squirrel-cage induction motor drive system that provides constant maximum torque or increased maximum torque and reduced slip speed at frequencies below the nominal frequency has been modeled, simulated and tested. Load performance analysis of the proposed system under different operation conditions was provided. These principles of operation are extended to the case of operation from variable frequency or variable voltage control method. Finally, the effects of the non-sinusoidal voltage and/or current wave shapes are covered.

The results show that both suggested improvement techniques (constant torque or constant flux) improve the steady-state performance A.C. drive system with squirrel cage induction motors. The slip speed has been decreased and the starting torque and maximum torque have been increased, which means that the suggested control techniques can be used in drive systems with short time operating mode under light loads.

Keywords: Induction Motor Drive, Constant Volts Per Hertz, Torque Speed Curve, dq Transformation, State-space Model.

Nomenclature:

v_{ds} = d-axis component of the stator voltage, V

v_{qs} = q-axis component of the stator voltage, V

i_{ds} = d-axis component of the stator current, A

i_{qs} = q-axis component of the stator current, A

i'_{dr} = d-axis component of the rotor current referred to the stator, A

i'_{qr} = q-axis component of the rotor current referred to the stator, A

V or V_s = stator voltage effective value

L_s = stator inductance, H

L'_r = rotor inductance referred to the stator, H

L_m = mutual inductance between rotor and stator, H

$L_{ss} = L_s + L_m$, H

$L'_{rr} = L'_r + L_m$, H

ω_s = stator electrical angular speed, rad/s

ω_r = rotor electrical angular speed, rad/s

$\omega_m = \frac{2}{P}\omega_r$, rotor mechanical angular speed, rad/s

P = number of poles

T_e = electromagnetic developed torque, N.m

T_m = load torque, N.m

J = equivalent moment of inertia, kg.m^2

1. INTRODUCTION

The three-phase squirrel cage induction motor is the most widely used motor type in the industry because of its good self-starting capability, simple and rugged structure, low cost and reliability [1-5]. In spite of this popularity, the induction motor has two basic limitations: (1) The standard motor is not a true constant-speed machine, its full-load slip varies from less than 1% (in high-horsepower motors) to more than 5% (in fractional-horsepower motors), and (2) It is not inherently capable of providing variable-speed operation [2,3]. Both of these limitations require consideration to meet quality and accuracy requirements of induction motor drive applications.

The limitations of induction motor can be solved through the use of adjustable speed control based on pulse width modulation techniques [4]. The basic control action involved in adjustable speed control of induction motors is to apply a variable frequency variable magnitude AC voltage to the motor to achieve the aims of variable speed operation [5]. Voltage source inverters and current source inverters are used in adjustable speed AC drives. However, voltage source inverters with constant Volts/Hertz (*V/f*) are more popular, especially for applications without position control requirements, or where the need for high accuracy of speed control is not crucial.

Ideally, by keeping a constant *V/f* ratio for all frequencies the torque-speed curve of induction motor can be reproduced at any frequency. In this case, the stator flux, stator current, and torque will be constant at any frequency [6]. The great majority of variable-speed drives in operation today are of this type although almost all research has been concentrated in field-oriented control theory, and little has been published about constant *V/f* operation. Its practical application at low frequency is still challenging, due to the influence of the stator resistance and the necessary rotor slip to produce torque [7].

In addition, the nonlinear behavior of the pulse-width modulated voltage-source inverter in the low voltage range makes it difficult to use constant *V/f* drives at frequencies below 3Hz [8, 9]. The performance of induction motor operating at constant *V/f* ratio can be improved by using different techniques, such as stator resistance compensation, slip compensation and vector compensation. The stator resistance compensation method consists of boosting the stator voltage by the magnitude of the current-resistance drop. Slip compensation results in increasing the operating frequency (speed). Vector compensation requires measurement of both voltage and current and accurate knowledge of machine inductances [10].

In this paper, two techniques to improve the performance of the inverter-induction motor drive system with constant *V/f* ratio controller are presented. The first technique is based on keeping the maximum torque constant for all operating frequencies, and equals to its value at nominal frequency. The second technique is based on maintaining the magnetic flux constant at all operating frequencies and equals to its nominal value. The proposed techniques are validated by simulation and experimental results. It is shown that large load torques are obtained, even in the low frequency range, with significantly reduced steady-state error in speed.

These principles of operation are extended to the case of operation from variable frequency and/or variable voltage control method. Finally, the effects of the non-sinusoidal voltage and/or current wave shapes are covered.

2. MODELING SYSTEM COMPONENTS

The block diagram of inverter-three-phase squirrel cage induction motor drive system is presented in figure 1. It consists of IGBT-inverter-based AC to AC converter, three-phase squirrel cage induction motor and controller. In order to analyze the system performance, all of these components should be modeled (mathematically described).

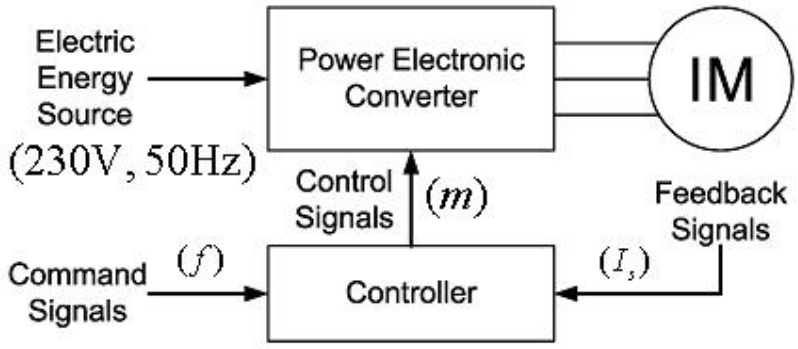

FIGURE 1: Block diagram of inverter-three phase squirrel-cage induction motor drive system

2.1. Modeling of the IGBT-Inverter-Based AC to AC Converter

The frequency converter is considered to be an ideal system, where the voltage at the dc side of the converter has no AC component. For sinusoidal pulse width modulation SPWM, the ratio of the amplitude of the sinusoidal waveform to the amplitude of the triangular waveform is called the modulation index *m*, which can be in the range of 0 to 1 [11]. The stator voltage V_s can be defined as:

$$V_s = m\, V_n \quad (1)$$

Where:

V_n = nominal value of stator voltage.

The frequency of the stator voltage *f* equals the frequency of the sinusoidal input waveform f_{in}.

$$f = f_{in} \quad (2)$$

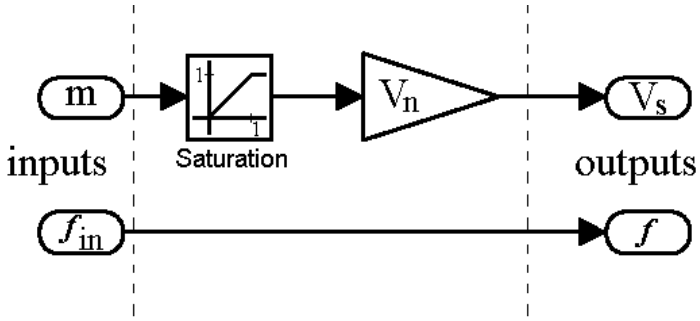

FIGURE 2: Steady-state model of inverter.

Varying the modulation index and the sinusoidal waveform frequency will change the RMS value of the stator voltage and frequency. Eqs. 1 and 2 constitute the steady-state model of inverter, shown in figure 2.

2.2. Modeling of Controller and Control Circuits

Based on the principle of *V/f* = constant, the controller must apply the following function:

$$m = \begin{cases} Kf, 0 < f < f_n \\ 1, \quad f \geq f_n \end{cases} \tag{3}$$

Where:

$K = 1/f_n$, and f_n = nominal frequency (50Hz). The block diagram of *V/f* = constant controller is shown in figure 3.

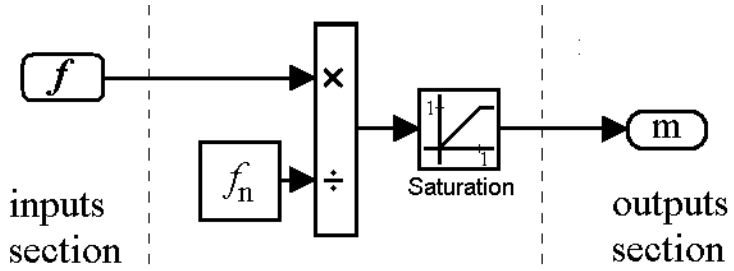

FIGURE 3: The model of *V/f* = constant controller.

Control circuits of A.C. drive system with induction motor can be divided according to different criterions. The following thinking will be focused on the fundamental properties of electric drives which are different from each other by the way of setting the required stator voltage of the motor:

1. **Variant 1:** The desired voltage may be measured and evaluated by using a suitable controller, "RI" shown in figure 4a.

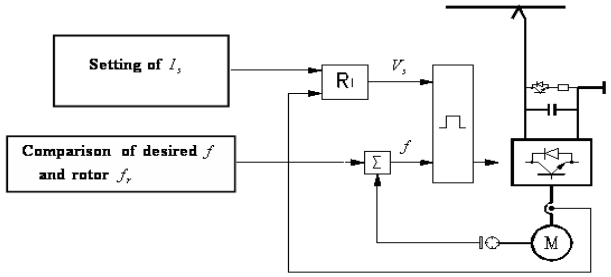

FIGURE 4A: Variant 1.

Under the effect of the variation of the load torque, the stator voltage may behave just like a disturbance that is applied to the control system. Therefore, if the current-controller, RI, is working well, then any change in the load torque will not affect the function of the motor which means that there is no need for a voltage feedback from the capacitor connected at the d.c. side of the rectifier as shown in figure 4a.

2. **Variant 2:** The stator voltage is simply estimated.

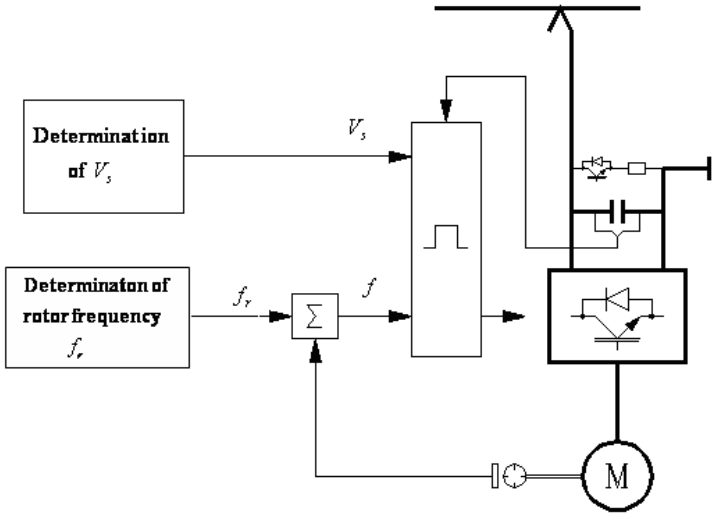

FIGURE 4B: Variant 2.

If the estimated voltage has to be equal exactly to the actual stator voltage even after it is changed, then it is necessary to take into consideration the voltage feedback from the capacitor as shown in Fig. 4b.

2.3. Modeling of Three-Phase Squirrel Cage Induction Motor

Many studies of the transient and steady state performance of induction motors have used two axes (d-q) dynamic machine model for the solution of the motor performance equations [12], while other studies have used a direct three-phase dynamic model that seemed more convenient, due to the variables involved in such modeling, in which they are the actual physical quantities of the motor [13]. Some authors have used dynamic model for small perturbations and transfer function, or solutions for dynamic behavior in complex symbolic form [14].

The steady state performances of the induction motors are obtained using static model

equations, derived from a dynamic model by setting their derivatives to zero and solving the resulting motor equations for the motor variables.

The state-space model of the squirrel cage three-phase induction motor in standard form, with respect to a synchronously rotating d-q coordinates, can be expressed as[15, 16]:

$$\left.\begin{aligned}\dot{\mathbf{x}} &= \mathbf{A}\mathbf{x} + \mathbf{B}\mathbf{u} \\ \mathbf{y} &= \mathbf{C}\mathbf{x} + \mathbf{D}\mathbf{u}\end{aligned}\right\} \quad (4)$$

Where the matrix quantities in Eq. 4 are as follows:

$\dot{\mathbf{x}} = \left[\dot{i}_{ds} \quad \dot{i}'_{dr} \quad \dot{i}_{qs} \quad \dot{i}'_{qr} \quad \dot{\omega}_m\right]^T$ -state equations vector

$\mathbf{x} = \left[i_{ds} \quad i'_{dr} \quad i_{qs} \quad i'_{qr} \quad \omega_m\right]^T$ -state vector

$\mathbf{Y} = \left[i_{ds} \quad i'_{dr} \quad i_{qs} \quad i'_{qr} \quad \omega_m \quad T_e\right]^T$ -output vector

$\mathbf{u} = \left[v_{ds} \quad 0 \quad v_{qs} \quad 0 \quad T_m\right]$-input vector

$\mathbf{D} = [0]$-direct transmission matrix

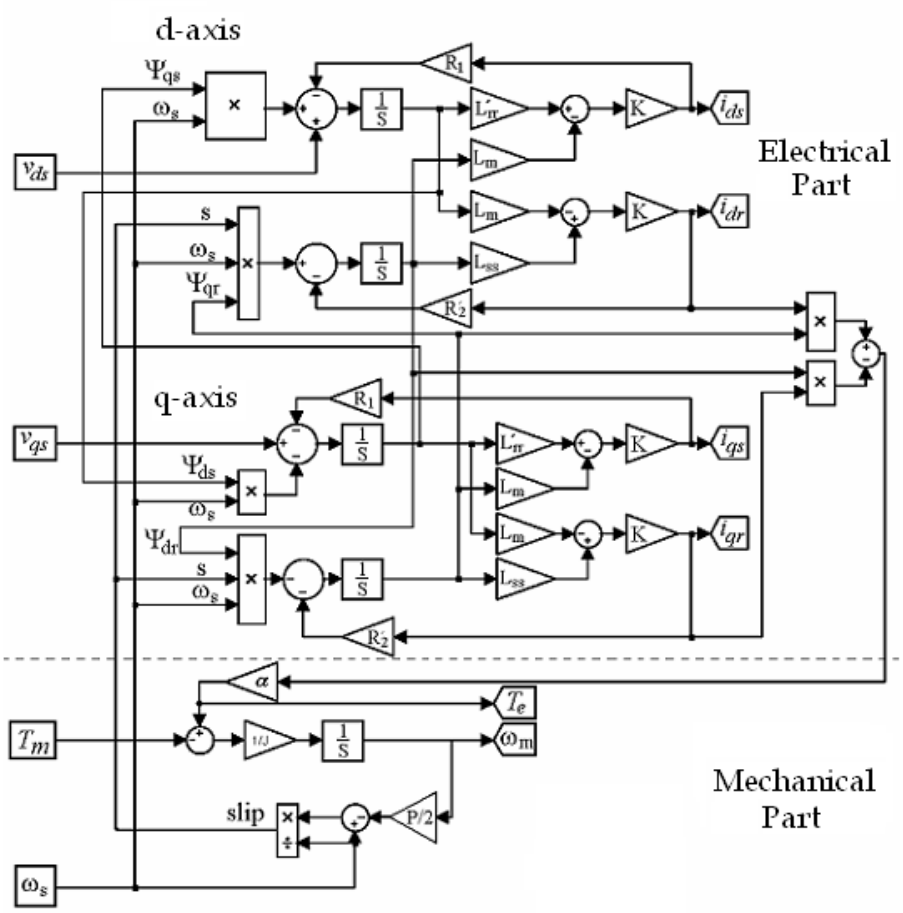

FIGURE 5: State-space model of induction motor.

$$\mathbf{A}=\begin{bmatrix} \omega_s+\frac{P}{2}\omega_m K_2 & \frac{P}{2}\omega_m K_1\frac{L_m}{L_{ss}} & \frac{R_1}{L_{ss}}K_1 & -\frac{R'_2}{L_m}K_2 & 0 \\ \frac{R_1}{L_{ss}}K_1 & -\frac{R'_2}{L_m}K_2 & -\omega_s-\frac{P}{2}\omega_m K_2 & -\frac{P}{2}\omega_m K_1\frac{L_m}{L_{ss}} & 0 \\ -\frac{P}{2}\omega_m K_1\frac{L_m}{L'_{rr}} & \omega_s-\frac{P}{2}\omega_m K_1 & -\frac{R_1}{L_m}K_2 & \frac{R'_2}{L'_{rr}}K_1 & 0 \\ -\frac{R_1}{L_m}K_2 & \frac{R'_2}{L'_{rr}}K_1 & \frac{P}{2}\omega_m K_1\frac{L_m}{L'_{rr}} & -\omega_s+\frac{P}{2}\omega_m K_1 & 0 \\ -\frac{\alpha L_m i'_{qr}}{J} & 0 & \frac{\alpha L_m i'_{dr}}{J} & 0 & 0 \end{bmatrix}$$ -state matrix

$$\mathbf{B}=\begin{bmatrix} \frac{K_1}{L_{ss}} & 0 & -\frac{K_2}{L_m} & 0 & 0 \\ 0 & \frac{K_1}{L_{ss}} & 0 & -\frac{K_2}{L_m} & 0 \\ -\frac{K_2}{L_m} & 0 & \frac{K_1}{L'_{rr}} & 0 & 0 \\ 0 & -\frac{K_2}{L_m} & 0 & \frac{K_1}{L'_{rr}} & 0 \\ 0 & 0 & 0 & 0 & -\frac{1}{J} \end{bmatrix}$$ -input matrix

$$\mathbf{C}=\begin{bmatrix} 1 & 0 & 0 & 0 & 0 \\ 0 & 1 & 0 & 0 & 0 \\ 0 & 0 & 1 & 0 & 0 \\ 0 & 0 & 0 & 1 & 0 \\ 0 & 0 & 0 & 0 & 1 \\ -\alpha L_m i'_{qr} & 0 & \alpha L_m i'_{dr} & 0 & 0 \end{bmatrix}$$ -output matrix

$\alpha=\frac{3}{4}P$ -constant; $K_1=\frac{L_{ss}L'_{rr}}{L_{ss}L'_{rr}-L^2_m}$ -constant; $K_2=\frac{L^2 m}{L_{ss}L'_{rr}-L^2_m}$ -constant

The model of mechanical part of an induction motor can be represented by:

$$T_e-T_m=J\dot{\omega}_m \tag{5}$$

Where the electromagnetic torque T_e is expressed as:

$$T_e=\frac{3}{4}PL_m(i_{qs}i'_{dr}-i_{ds}i'_{qr}) \tag{6}$$

Inputting Eq. 8 into Eq. 7, we get:

$$\dot{\omega}_m=\frac{3}{4}\frac{PL_m}{J}i_{qs}i'_{dr}-\frac{3}{4}\frac{PL_m}{J}i_{ds}i'_{qr}-\frac{1}{J}T_m \tag{7}$$

The state-space model of induction motor as electromechanical system is shown in figure 5. The parameters of simulated induction motor are given in table 1. The block diagram of the drive system studied using MATLAB Simulink is shown in figure 6.

It was noticed also that the absolute slip decreased by decreasing the frequency. The absolute slip defined as:

$$s_a = \frac{\omega_0 - \omega_m}{\omega_{0n}} \tag{8}$$

Where:

ω_0 is the no-load speed at a given frequency and ω_{0n} is the no-load at nominal frequency.

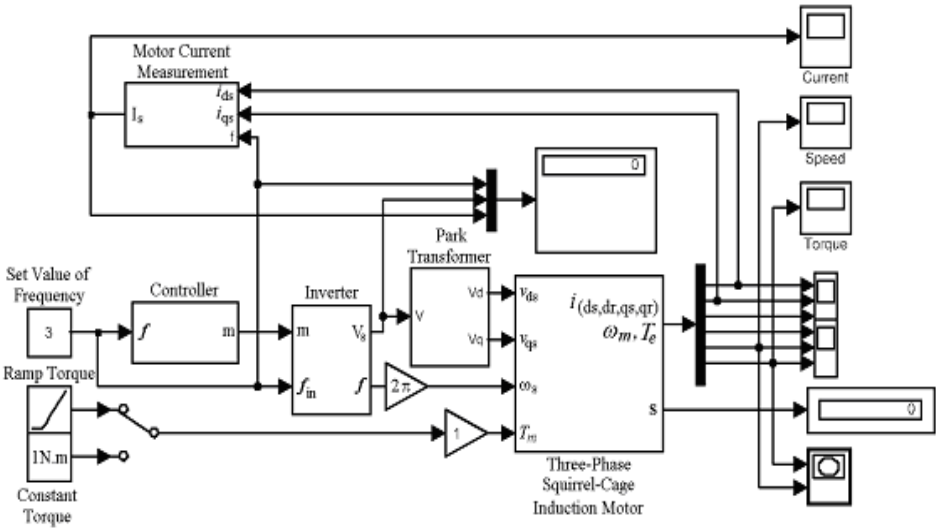

FIGURE 6: The model of the drive system.

2.4. Control With Constant Maximum Torque

The maximum torque at nominal frequency $T_{\max(n)}$ can be determined by the following equation [10]:

$$T_{\max(n)} = \frac{3PV^2 n}{8\pi f_n (R_1 + \sqrt{R^2{}_1 + X^2{}_{syn}})} \tag{9}$$

Where:

V_n = nominal value of stator voltage (phase), f_n = nominal frequency, and

$X_{syn} = X_1 + X'_2 = 2\pi f_n (L_s + L'_r)$

The maximum torque $T_{\max}$ at any frequency *f* can be determined as:

$$T_{\max} = \frac{3PV^2}{8\pi f (R_1 + \sqrt{(R^2{}_1 + (2\pi f L_s + 2\pi f L'_r)^2)})} \tag{10}$$

Equating Esq. 9 and 10, we get:

$$m = \frac{V}{V_n} = \frac{V_s}{V_n}\frac{f}{f_n}\sqrt{\frac{\frac{f_n}{f}R_1 + \sqrt{(\frac{f_n}{f})^2 R^2{}_1 + X^2{}_{syn}}}{R_1 + \sqrt{R^2{}_1 + X^2{}_{syn}}}} \tag{11}$$

Equation 11 shows that the value of the modulation index m generated for the controller with constant maximum torque is greater than that generated for the controller with $V/f = \text{constant}$. The model of $T_{\max} = \text{constant}$ controller is shown in figure 7.

The simulated mechanical characteristics of the drive system with $T_{\max} = \text{constant}$ controller are shown in figure 8, from which it is clear that the maximum torque remains constant for the

frequency range from 20Hz up to 50Hz. For frequencies below 20Hz the maximum torque has been significantly increased comparing with that of the drive system with $V/f = \text{constant}$ controller. The absolute slip has been decreased.

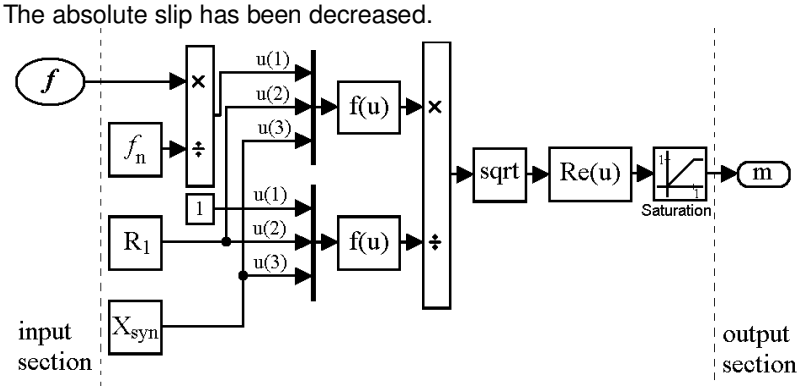

FIGURE 7: The model of $T_{\max} = \text{constant}$ controller.

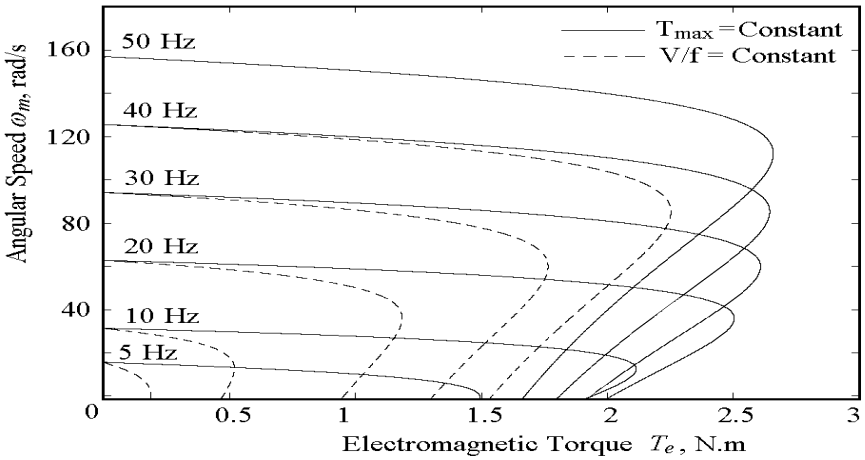

FIGURE 8: Mechanical characteristics of drive system with T_{max}= constant controller

Parameter	Value
Stator resistance R_1	65
Stator reactance X_1	40
Mutual reactance X_m	241
Rotor resistance referred to the stator R'_2	25
Rotor reactance referred to the stator X'_2	30
Nominal voltage V_n	230/400V
Nominal torque T_n	1.3N.m
Nominal input power P_n	0.25kW
Nominal current I_n	0.76A
Power factor	0.79
Nominal frequency f_n	50Hz
Number of poles P	4
Nominal speed n_n	1455 rpm
Nominal angular speed	152 rad/s
Moment of inertia J	0.02 kg.m^2

TABLE 1: Motor parameters

2.5. Control With Constant Flux

The stator flux can be kept constant, and equal to its nominal value, if the ratio of the magnetizing e.m.f. E_m to the stator frequency f remains constant, $(\frac{E_m}{f} = \frac{E_{mn}}{f_n})$. Under this condition, and based on the induction motor steady-state equivalent circuit and phasor diagram, the stator voltage V can be determined as:

$$V = K_{V/f} + R_1\sqrt{I^2{}_s - I^2{}_m} \quad (12)$$

Where:

$K_{V/f} = \frac{V}{f} = \text{constant}$, I_m = magnetizing (no-load) current.

Eq. 12 shows that the stator voltage V in the case of controller with constant flux is always greater than that of $V/f = \text{constant}$ controller. The model of controller with constant flux is shown in figure 9.

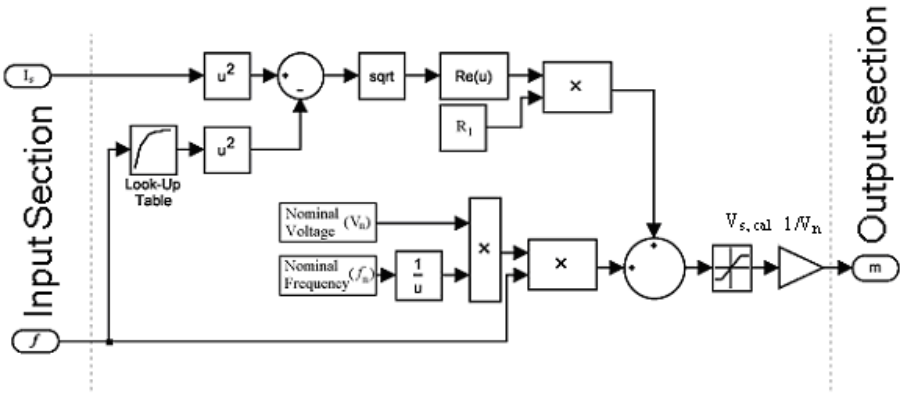

FIGURE 9: The model of ϕ = constant controller.

3. SIMULATION RESULTS

The Performance analysis of the drive system with V/f controller was provided for different values of frequency and load torque. The magnetization curve of the motor is given as follows:

$$\Psi_h = f(I_m): \begin{matrix}(I_m : \psi_h) = 0,0,29,0.24,39,0.31,60,0.38,63,0.45,80,0.5, \\ 101,0.56,132,0.63,151,0.7,\ 229,0.76,\ 311,0.83,\ 422,0.9,\ 576,0.96\end{matrix}$$

Examples of dynamic response of the system are shown in the following figures. Simulated mechanical characteristics of the drive system with different types of controllers are represented in figure 10, which shows that decreasing the frequency causes a significant increase in the maximum torque in the case of a controller with constant flux.

Figure 11 shows that the absolute slip is reduced and less than that of other types of controllers. The obtained mechanical characteristics of the drive system with constant flux controller are similar to those of drive system operating with constant power.

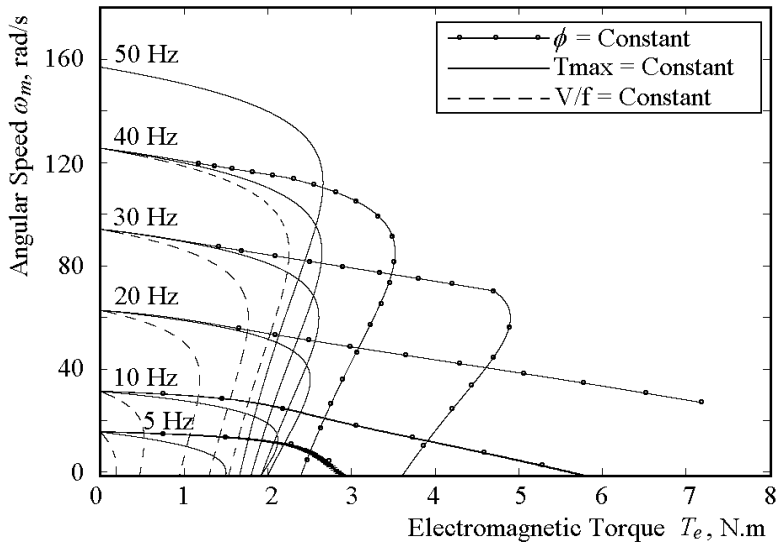

FIGURE10: Mechanical characteristics of drive system with different types of controllers.

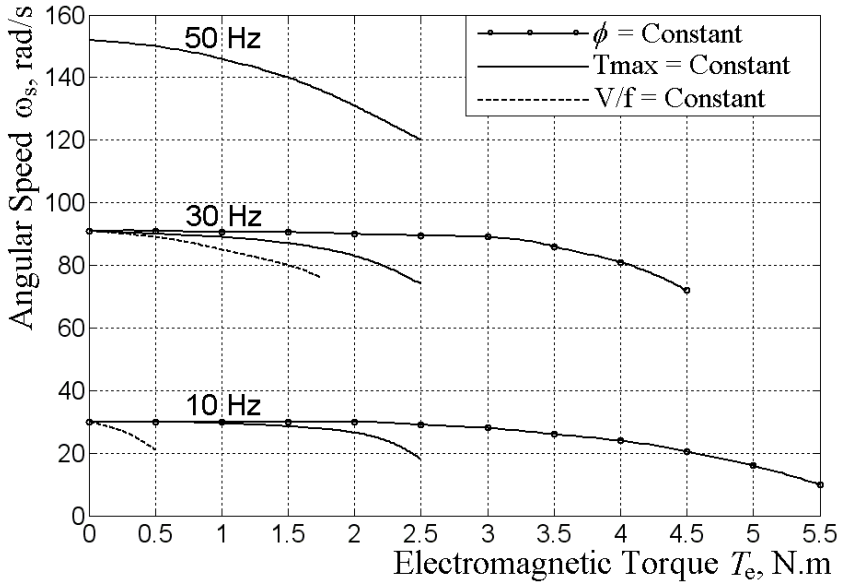

FIGURE11: Experimental mechanical characteristics of drive system with different types of controllers.

Figure (12) shows the plot of the stator voltage space vector versus the stator current space vector, $\mathbf{U_s}$ versus $\mathbf{I_s}$, the plot of the developed torque, T_e, and the *r.m.s.* value of the stator current, I_{sef} versus the rotor frequency, f_r.

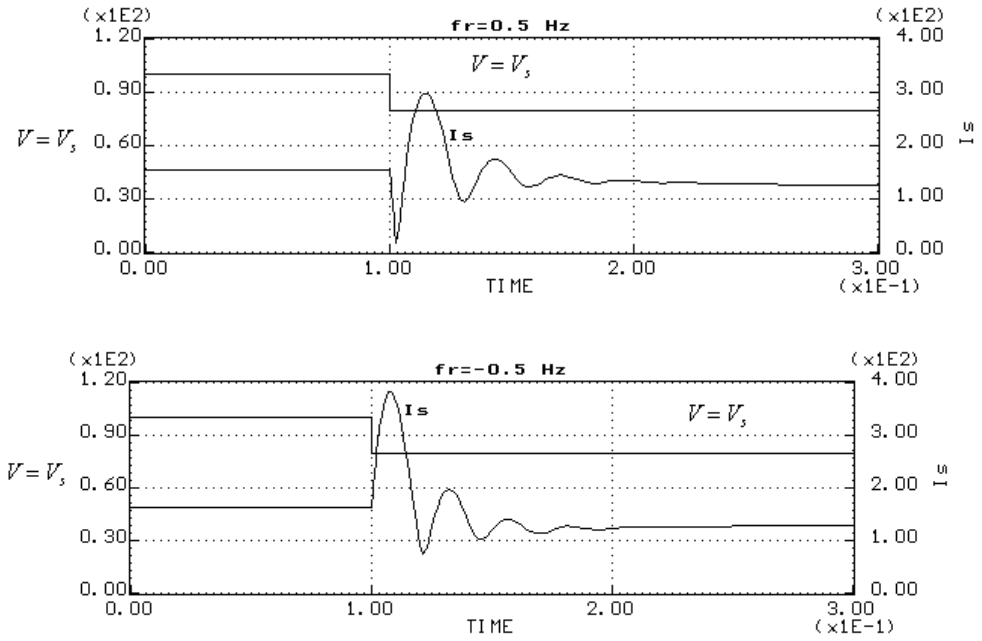

FIGURE 13: a plot of (a) V_s, I_s …abs. value of space vectors in time domain

Figure 13 shows the stator voltage and current space vectors, $\mathbf{U_s}$ and $\mathbf{I_s}$, under the condition of a variable stator voltage and constant rotor frequency. The response of the system on a change in the stator voltage while the rotor frequency is constant is adversely bad.

The results show that both the absolute value of the space vector of the stator current and the motor torque, T_e, increase with the increasing rotor frequency. The motor was not able to start at frequencies below 22Hz at load of 1.0N.m and below 11Hz at load of 0.5N.m. It was noticed also that the absolute slip, defined as $s = \frac{\omega_0 - \omega_m}{\omega_{0n}}$, is decreased with the decreasing frequency, where ω_0 is the no-load speed at a given frequency and ω_{0n} is the no-load at nominal frequency. Variation of frequency does not have significant effect on the steady-state value of stator current. Similar results were reported in [10, 11].

Therefore, if the voltage is set at the output of the controller (e.g. current), then it will cause some serious problems: during breaking regime and after reducing the voltage as it is seen in figure 13, an overshoot in the stator current is generated which is considered to be a currently known phenomenon. It could be explained by using an equivalent schematic diagram which respects the induced voltage in the stator circuit, $\frac{d\psi}{dt}$ and that in the rotor circuit, $\frac{1}{s}\frac{d\psi}{dt}$.

The simulation in figure 14 is carried out for a variable rotor frequency and constant voltage. The response to a step change in the rotor frequency is completely trouble free as it is shown in the figure. The frequency of the rotor may easily be evaluated by using a controller of any quantity, for example (e.g. Siemens, Simovert P … f_r is evaluated by using a controller of the torque component).

In order to improve the starting and load performance of the drive system under the effect of stator voltage variations, a filter is added at the output of the current controller which may have a bad effect on the dynamic properties of the current loop, especially if the loop contains further blocks with expected delay in the response. Therefore, the stator voltage V_s is set using a limiter at the output of the controller and a PI controller (K_{RI}, T_{RI}) must be added as

shown in figure 15. When the voltage decreases, the PI controller reduces the firing angle. When the voltage increases, the PI controller increases the firing angle.

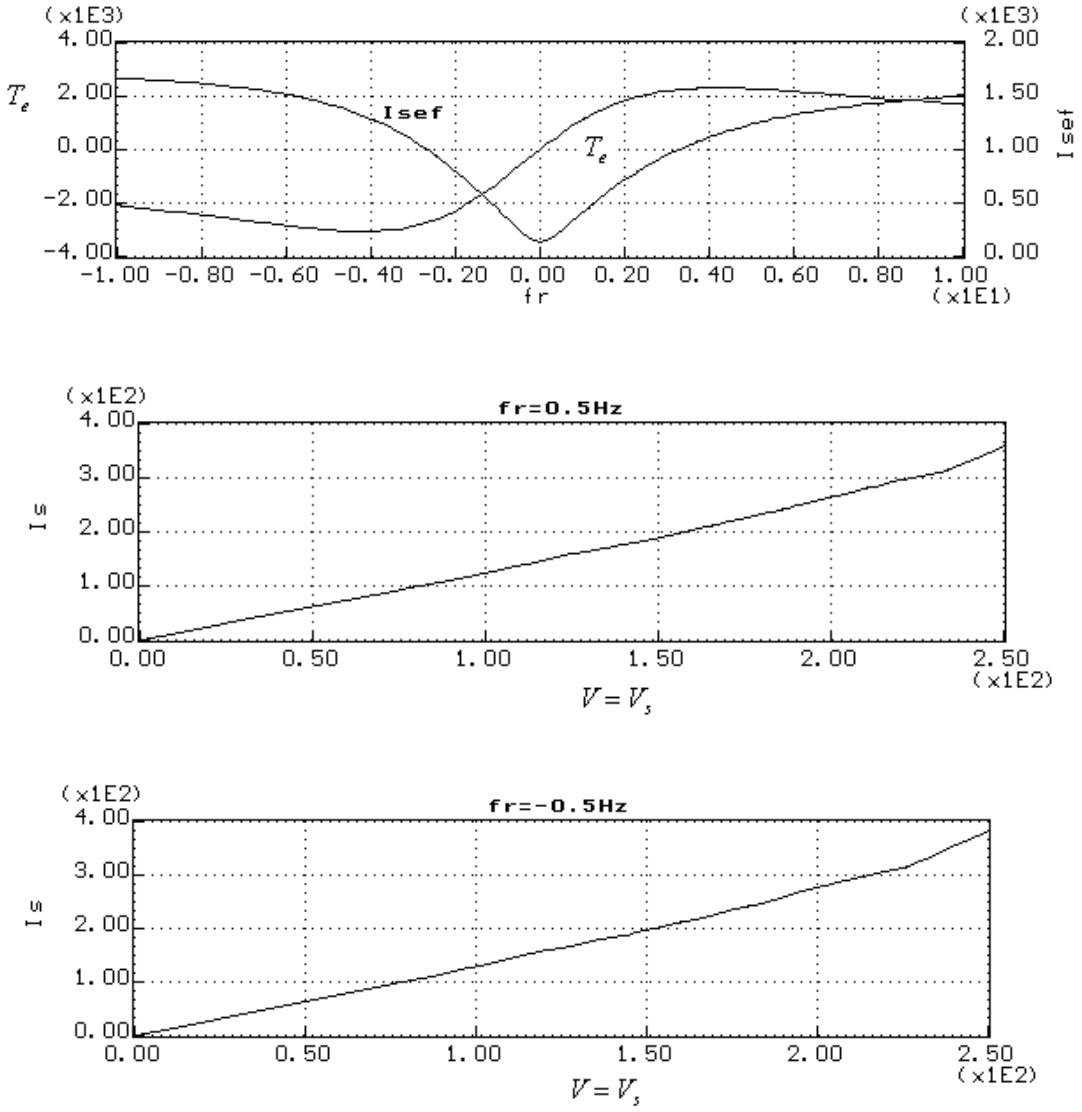

FIGURE 12: a plot of : (a) torque T_e versus rotor frequency. (b) V_s versus Is …absolute values of space vectors.

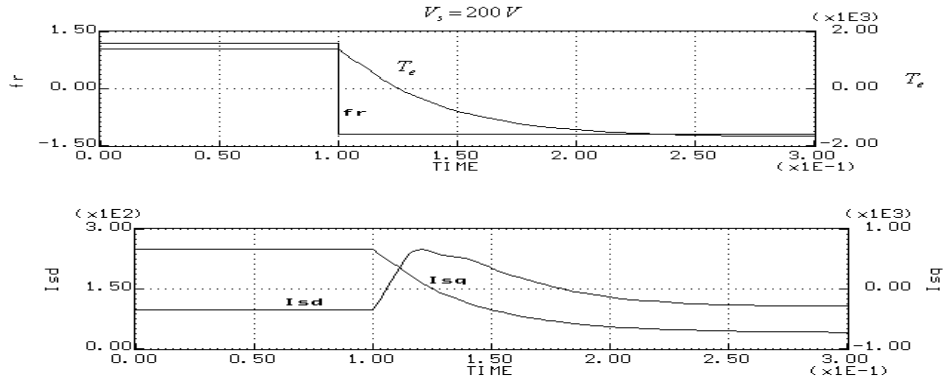

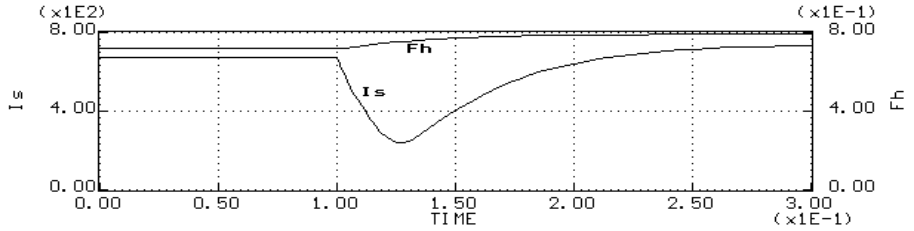

FIGURE 14: I_{sd}, I_{sq} … direct and quadrature components of stator current vector, T_e … developed torque, F_h …magnetomotive force.

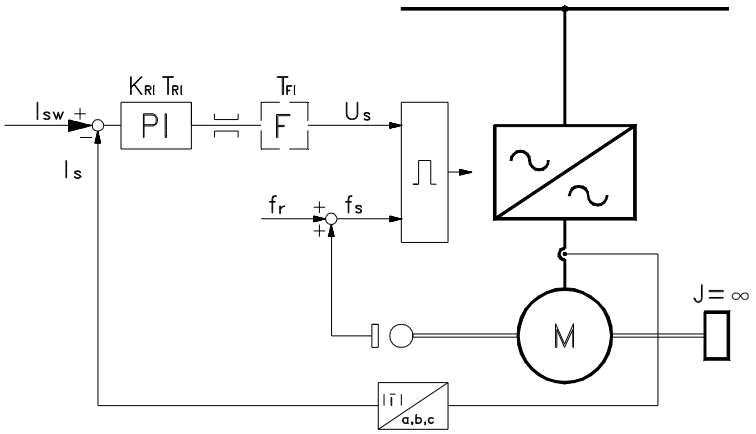

FIGURE 15: Improved control schematic topology

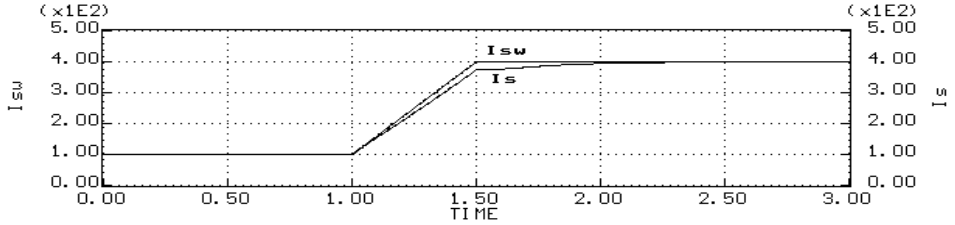

fr = 0.6 Hz, ω=2.π.40, K_{RI} = 2, T_{RI} = 0.2 s, T_{FI} = 0, I_s …absolute values of space vectors.

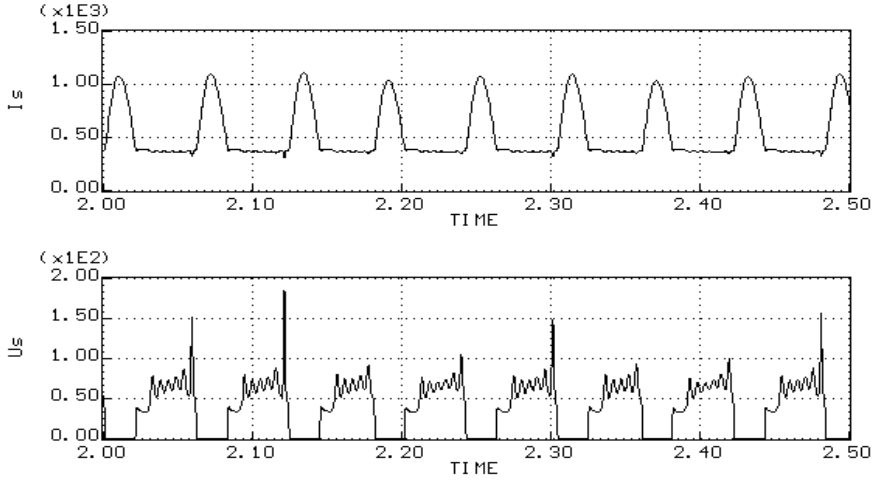

f_r = -0.6 Hz, ω=2.π.40, K_{RI} = 2, T_{RI} = 0.2 s, T_{FI} = 0.

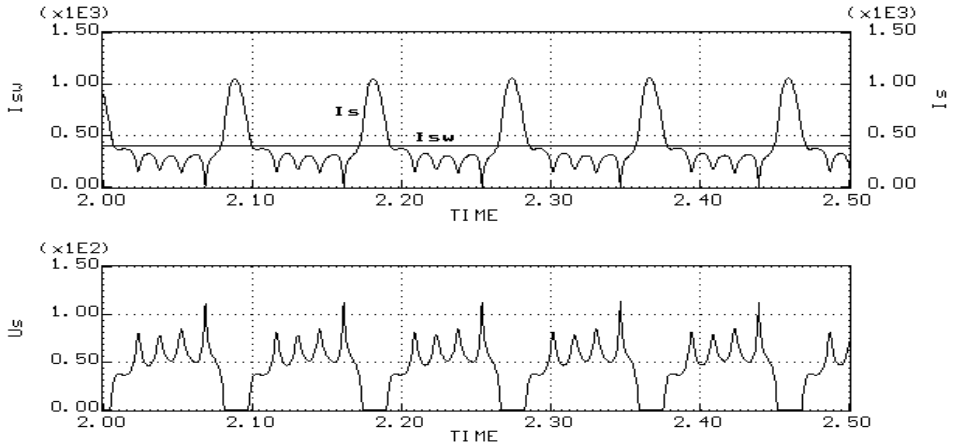

f_r = -0.6 Hz, ω=2.π.40, K_{RI} = 0.2, T_{RI} = 0.5 s, T_{FI} = 0, (small gain , without a filter).

FIGURE 16: Improved simulation results, Isw: desired r.m.s. value of I_s.

In the AC motor drive, the motor speed is not regulated in closed loop. Instead, the speed set point is used only to determine the motor voltage and frequency applied by the six-step inverter in order to maintain the (*V/f*) ratio (or the motor flux) constant from 0 to the nominal speed. Above nominal speed, the motor operates in the flux weakening mode; that is, the voltage is maintained constant at its nominal value while the frequency is increased proportionally to the speed set point. When reversing speed, a short delay is required at the zero speed crossing so that air gap flux decays to zero.

Under the above mentioned improvement conditions, figure 16 shows an improved simulation carried out for different values of rotor frequency and controller parameters.

4. CONCLUSION

Based on the results obtained in this paper, the following conclusions can be made:

1. The derived state-space model of three-phase squirrel cage induction motor can be used to analyze the performance of induction motor drive systems.
2. The implementation of constant maximum torque and constant flux controllers improves the performance of inverter-induction motor drive systems.
3. The mechanical characteristics of the drive system with constant flux controller are harder than that with constant maximum torque controller.
4. It is recommended to use constant maximum torque controller in drive systems operating with constant torque.
5. It is recommended to use constant flux controller in drive systems operating with constant power.

5. REFERENCES

[1]. R.W. De Doncker, D. W. Novonty. "The Universal Field Oriented Controller," IEEE Trans. Ind. Applicat., vol. IA-30, No 1, 1994, pp. 92-100.

[2]. R.D. Lorentz, T.A. Lipo and D.W. Novotny. "Motion Control with Induction Motors," Proceedings of IEEE, vol. 82, No. 8, 1994, pp. 1215-1240.

[3]. O.I. Okogo. "MATLAB Simulation of Induction Machine with Saturable Leakage and Magnetizing Inductances," The Pacific Journal of Science and Technology, vol. 5, No. 1, April 2003 (Spring), pp. 5-15.

[4]. A.E. Fitzgerald. " Electric Machinery," 5th Ed., McGraw-Hill, 1990.

[5]. R. Gabriel, and W. Leonhard. "Microprocessor Control of Induction Motor," IEEE/IAS Int. Sem. Power Conv. Conf. Rec., 1982, pp. 385-396.

[6]. R. Marino, S. Peresada, and P. Valigi. "Adaptive Input-Output Linearizing Control of Induction Motors," IEEE Trans. Autom. Cont., vol. 38, No. 2, 1993, pp. 208-221.

[7]. Hussein Sarhan, Rateb Al-Issa, and Qazem Jaber. "Loss-Minimization Control of Scalar Controlled Induction Motor Drives," 4th IEEE GCC Conference and Exhibition, Manama, Kingdom of Bahrain, 12th-14th Nov., 2007, p. 64.

[8]. K. Zhou and D. Wang. "Relationship Between space-Vector Modulation and Three-phase Carrier-Based PWM: A Comprehensive Analysis," IEEE Trans. Ind. Electronics, vol. 49, No. 1, 2002, pp. 186-195.

[9]. B.K. Bose. "Power Electronics and Variable Frequency Drives," IEEE Press, 1997, p. 402.

[10]. M.G. Alfredo, A.L. Thomas, and W.N. Donald. "A New Induction Motor V/f Control Method Capable of High-Performance Regulation at Low Speeds," IEEE Trans. Ind. Applicat., vol. 34, No. 4, July-august, 1998, pp. 813-820.

[11]. R. Sepe and J. Lang. "Inverter Nonlinearities and Discrete-Time Vector Current Control," IEEE Trans. Ind. Applicat., vol. 30, Jan.-Feb., 1994, pp. 62-70.

[12]. M.A. Ouhrouche. "Simulation of Direct Field-Oriented Controller for an Induction Motor Using MATLAB-Simulink Software Package," Proceedings of the IASTED International Conference Modeling and simulation, May 15-17, 2000-Pittsburgh, Penn sylvania, USA.